Optimization based exploitation of the ankle elasticity of HRP-2 for overstepping large obstacles

Kai Henning Koch, Katja Mombaur, Olivier Stasse, Philippe Souères

Optimization based exploitation of the ankle elasticity of HRP-2 for overstepping large obstacles

Kai Henning Koch[1] Katja Mombaur[2] Olivier Stasse[3] Philippe Souères[4]

***Abstract*— This paper proposes a new generic strategy to investigate the dynamic limits of the humanoid robot HRP-2 based on whole body optimal control optimization. In this study we exploit the intuitive access to complex motion characteristics, given by optimal control, to effectively resolve a major technical coupling effect, namely between the ankle elasticity and the stabilizing algorithms. Control efforts are reduced to get a clearer view of the actual system limits and to exploit its capacities at maximum. As showcase we decided to focus on a stepping motion over a cylindrical obstacle.**
This study is further supported by real experiments on the HRP-2 14 robotic platform and we could successfully extend the present maximum of a dynamically overstepped obstacle to 20cm (height) x 11cm (width) (including safety margin) without multi-contact support.

I. INTRODUCTION

While humanoid robots are some of the most exciting machines in the world, they come at the same time with a highly complex design of its overall system architecture. At one hand this complexity is essential to the capacity of bipedal locomotion (e.g. redundancy & under-actuation). At the other hand, it poses further difficulties as soon as one tries to investigate or even improve its motion characteristics towards more human-like/natural locomotion trajectories.
Even though Humanoid robots have been conceived in the hope to efficiently exploit the advantage of bipedal locomotion to robustly cope with irregular terrain conditions, these robots are eventually struggling with serious problems, as soon as it comes to more challenging situations like, stepping over large obstacles. The possibility to overcome large obstacles is a particular advantage of legged, and especially bipedal systems over their wheeled counterparts. Limitations to a flexible and robust operation for these robots are at some point certainly related to the given hardware and the control system. Besides, some limits may as well originate from the employed algorithms for motion generation and the technological inter-dependencies between control system and the underlying hardware. As some of the frequently employed well-performing algorithms for computing stepping trajectories are very conservative, full exploitation of the capabilities of hardware and control system may not be possible at some point.

[1]henning.koch at iwr.uni-heidelberg.de
[2]katja.mombaur at iwr.uni-heidelberg.deORB Optimisation in Robotics and Biomechanics, IWR University of Heidelberg, INF 368, 69120 Heidelberg, Germany
[3]ostasse at laas.fr
[4]psoueres at laas.frGEPETTO, LAAS-CRNS TOULOUSE, avenue du Colonel Roche 7, 31031 Toulouse cedex 4, France

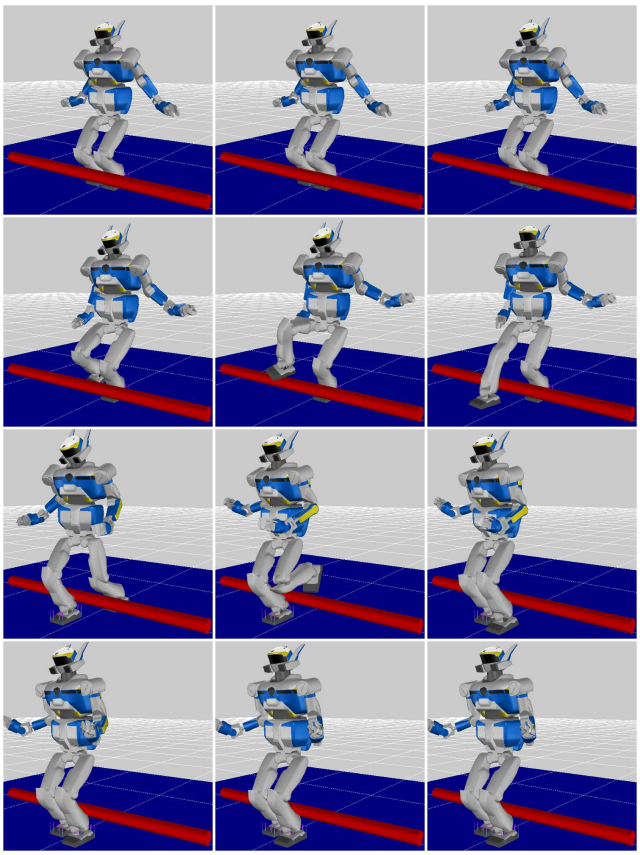

Fig. 1. image sequence of the stepping motion

A. Related research

The research field of motion generation based upon a physical model - more specifically walking motions (see [23]) - has the common target to efficiently identify the most suitable motion trajectory, among a sub-manifold of feasible candidate solutions, with the desired characteristics (e.g. stability). Depending on the desired characteristics of the final generation algorithm one may adopt different simplifications (e.g. on the physical model - inverted pendulum [7]) and heuristics to lower the complexity of the generic problem formulation.
On one hand, a very successful heuristic method for stable walking motions is the ZMP-based [21] pattern generation [7]. From a desired ZMP trajectory and planned footsteps, based on a simplified model (e.g. 3D-LIPM), one may compute the trajectory of the center of mass and, with further assumptions, the whole body motion (e.g. by inverse

Fig. 2. image sequence of the stepping motion

kinematics or resolved momentum control). Apart from the ZMP based pattern generation, Englsberger et. al. [5] have introduced a method featuring the capture point. Most of these pattern generators are easily parametrized, re-actively controllable, but are implicitly bound to the previously made assumptions in form of model-simplifications and heuristics. How these limitations finally translate to the resulting motion is however not always clear.

On the other hand, optimization based approaches keep a more generic form of the problem formulation. In consequence their solution generally involves the efficient computation of non-linear programming problems. Thus the high mathematical complexity of these approaches does not permit motion generation in real-time, but gives a more intuitive access to desired motion characteristics based on high-level objectives. Early works on gait cycle optimization based on forward dynamics of whole body optimal control have been conducted by [14]. Mombaur et.al. [15] investigated human-like running based on whole body optimal control using multiple shooting techniques. The stack of tasks [11] is a highly efficient whole body dynamics motion generation method with task prioritization. Erez et.al [19] generates running gaits based on inverse dynamics under external contacts.

Since bipedal locomotion devices are meant to move around in unstructured environment, various approaches exist to clear obstacles with humanoid robots (e.g. ASIMO [13] and HRP-2 [22], [2]). Guan et. al. [22] conducted a kinematic feasibility analysis of obstacles to be overstepped concluding on a maximum obstacle of 24.21cm x 5cm (Width x Height). Dynamic overstepping was then achieved in [2] as part of a walking pattern, in simulation and real experiment pushing the maximal values to 18cm x 11cm (Width x Height) including a safety margin of 3cm. The motion is planned for feet and hip (including twist) trajectories from a previous geometric feasibility analysis. The whole body motion is then generated based on the powerful ZMP preview control pattern generator from Kajita et.al.[7].

Apart from the general on-line or off-line motion generation process a very difficult task is to stabilize the humanoid robot in real-time against external perturbations during the actual motion performance. In all robots from HRP (Humanoid Robotics Project) this on-line control component is called the stabilizer [17] and accomplishes most commonly a posture and a force control loop. The control component adjusts the reference joint angle trajectories such that, the desired posture reference coincides with the on-line estimation from the Kalman filter and the measured ground contact reactions follow the given ZMP reference. The force control is achieved by combination of the position controlled joints with a passive elasticity device [16] and a force torque sensor forming a feedback loop that is adjusted for maximal backdriveability. The same device acts in parallel as low-pass filter to reduce shock effects from foot to ground impact [18]. From the viewpoint of motion performance the complete system mostly operates as if the elasticity would not be present [2].

B. Contribution of this article

This article proposes a new approach based on whole body optimal control to investigate the potential limits for dynamically highly challenging motions. It is based on the common idea that, in case one would like to push the robot to its dynamic limits, the stress on the control system should by minimized. In consequence a candidate solution should be computed such that particularly the control action of the stabilizer is minimal. In this respect, the control system should be able to operate safely, despite perturbations, originating from model deficiencies and the external environment.

The concept is applied to the dynamically, highly challenging case of overstepping obstacles with the robotic platform HRP-2, performing only two steps and with a static posture as initial and final boundary condition. The problem is formulated as multi-phase optimal control problem, based on the whole body dynamic model, including all limitations on joint angle ranges, velocity as well as the actuation systems. Furthermore abstract criteria such as dynamic stability and intensity of stabilizing control actions are considered. The solution is solely based on the governing physics - any other information such as phase timing and joint angle trajectories are computed during the process and do not need to be specified in advance.

Finally the strategy is verified with motion experiments on

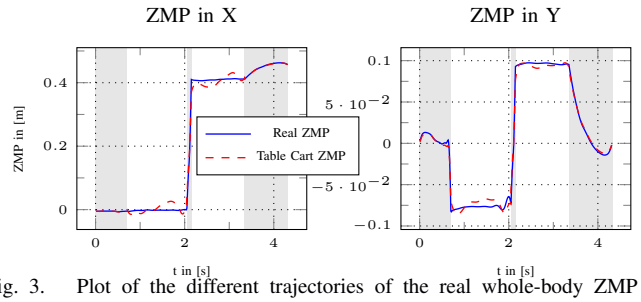

Fig. 3. Plot of the different trajectories of the real whole-body ZMP and the highly simplified table cart ZMP frequently used for stable motion generation of humanoid robots.

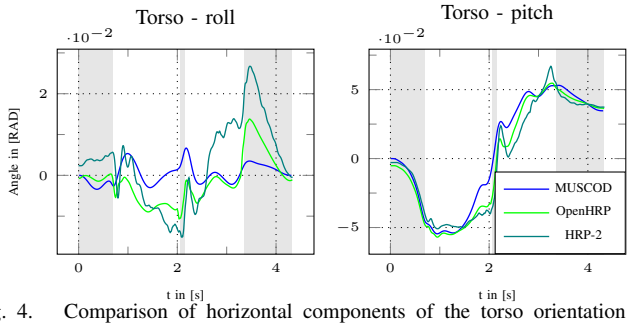

Fig. 4. Comparison of horizontal components of the torso orientation that are computed during optimization (MUSCOD), and estimated in the simulation of the virtual robot (OpenHRP), as well as during the experiment on HRP-2. Whilst the roll angle shows higher deviations the pitch orientation follows nicely the optimization results.

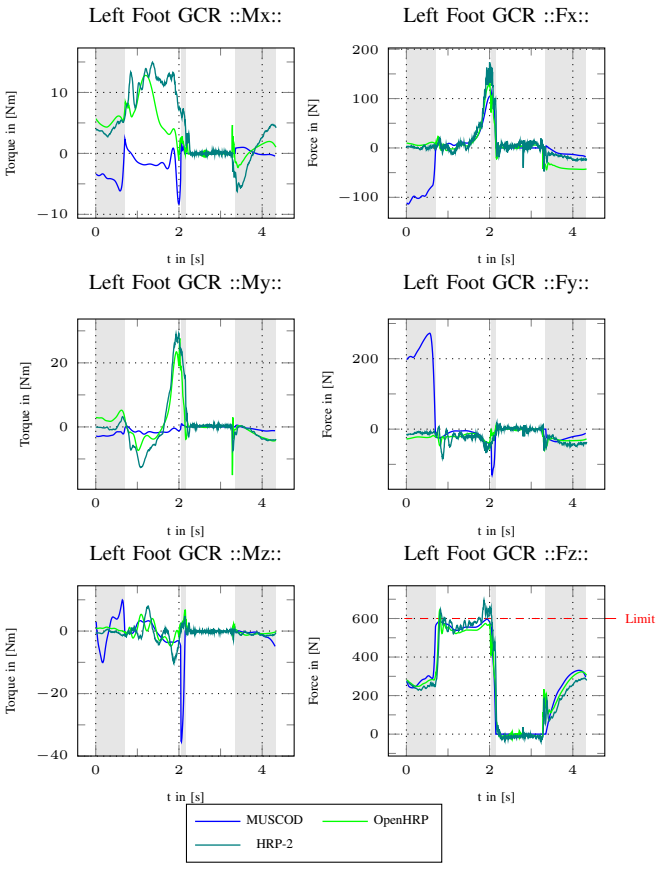

Fig. 5. Comparison of the left foot ground contact reactions for optimization results (MUSCOD), the simulation of the virtual robot (OpenHRP), as well as during the experiment on HRP-2. Close trajectories are observable for the contact forces Fx,Fy, Fz (vertical force) and the Mz (vertical torque). The stabilizing algorithms manipulate the components Mx, My as well as Fz. The vertical force limit should be kept firmly, however small peaks are not a problem.

the real robotic platform HRP-2 14 of LAAS-CNRS in Toulouse.

II. Modeling

A. Dynamic Modeling of the robot HRP-2

Despite the fact that the use of any robot with a sufficiently accurate model is possible, the chosen robotic platform for this analysis is the HRP-2 14. Technical information is given in [9]. As it is essential to modeling in optimal control that simplifications are carefully chosen to preserve the governing physical characteristics at maximum - a detailed outline is given below:

The robot HRP-2 [9] is controlled by high gain position control driving brushed DC motors through gearboxes with a high reduction ratios. As the position control carefully rejects external perturbation the joint trajectory reference governs the motion characteristic, while the torque profile only gives an estimation about the mechanical energy characteristics. Thus dry and viscous friction representing an offset to the torque profile is not considered. The reduction ratios are sufficiently high to neglect dynamic coupling of the rotor inertia and the kinematic structure. Further decision was made to assume the gearbox as perfectly rigid to reduce mathematical complexity.

In contrast to its predecessors [4] the kinematic structure of the robot has been conceived for maximum stiffness [9] and mass concentration in the pelvis (hosting the batteries). Consequently the kinematic structure is assumed perfectly rigid.

The feet of the robot are rubber coated [18] and mounted with elastic bushings underneath a 6D force sensor to the ankle joint complex. While the elastics of the rubber coating are mostly negligible, the ankle elasticity mechanism [16], [17] serves not only as shock absorber during bipedal locomotion. It is the physical component of the force torque control loop, built on top of the underlying joint position control loop to track the ZMP [21] reference for dynamically stable operation. The employed two DOF torque controller [16] is optimized for maximum backdriveability, hence distortion free frequency response for the reference signal is only guaranteed in low frequency space. Hence the elasticity is modeled as 2D rotational spring/damper system. The vertical elasticity effect will be neglected during this analysis for the sake of simplicity.

The previously mentioned control system is part of a stabilizing algorithm that accomplishes the following tasks [17]: Control of the pelvis postures based on the estimation of the orientation from the IMU in the upper torso and heuristics-based distribution of the vertical force on both feet as well as the contact torque. Torque and vertical force are directly related to the local CoP and the ZMP as long as the feet are firmly placed on the ground [21]. The control reference is

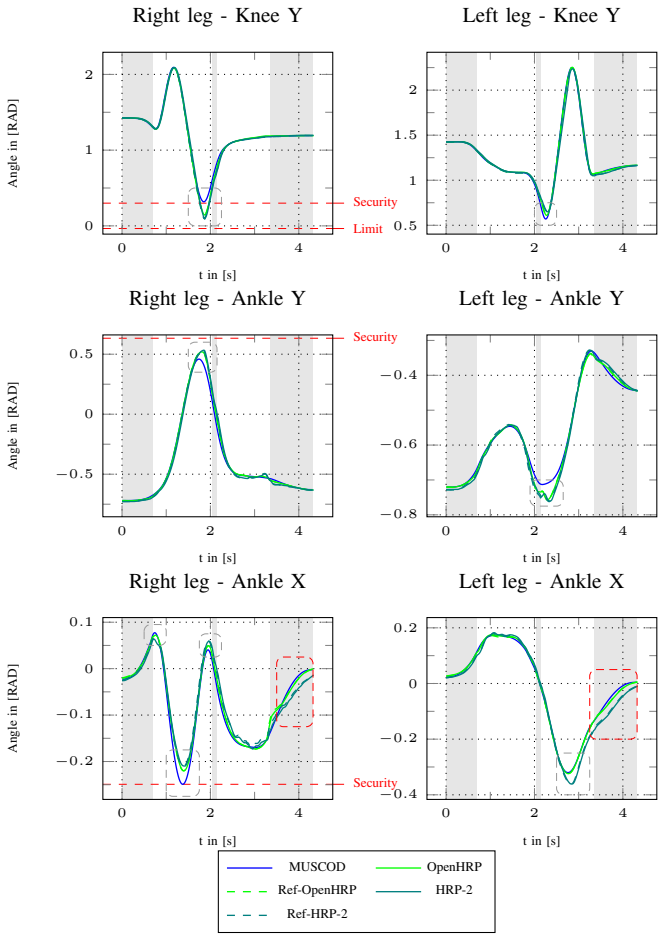

Fig. 6. Comparison of some joint trajectories for the lower torso part, for optimization results (MUSCOD), the simulation of the virtual robot (OpenHRP), as well as during the experiment on HRP-2. The control reference (scattered line) and the system's output (solid line) are drawn separately for verification. The limit marks the absolute maximum angle range for the corresponding joint. The security limit was the actual limit chosen during the optimization to enforce safe operation. The dashed gray/red rectangle show parts of the trajectory where the stabilizer actively manipulated the motion to preserve dynamic stability. In red rectangles even the simulation and the real robot act substantially different.

obtained from the dynamics of the linear inverted pendulum [17]. In the former variant the angular momentum change of the body is not considered for control. The correction of the trajectory profile is distributed over the lower body by means of inverse kinematics while turning around the CoM of the robot [8]. As it is not clear which of the present stabilizer variants is currently implemented on HRP-2 14, the most probable and constraining option is considered for this analysis.

B. Stepping over motion

The generation process is formulated as multi-phase hybrid dynamic, optimal control problem with continuous, as well as discontinuous phase transitions (see figure 1, sequence 1-12 left-right/top-down):
The motion initiates from a static posture towards unloading the right foot (1-3, highlighted in grey). The right foot lifts off ground and travels over the obstacle (4-6). Following the

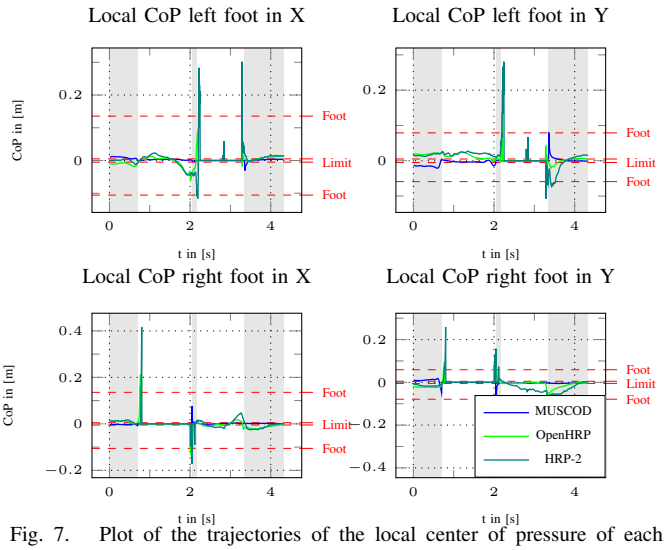

Fig. 7. Plot of the trajectories of the local center of pressure of each foot in X and Y for optimization results (MUSCOD), the simulation of the virtual robot (OpenHRP), as well as during the experiment on HRP-2. High peaks occur during the transition phase caused by the vertical contact force dropping to 0. The mark *foot* represents the physical boundary of the foot. As soon as the CoP reaches this boundary the contact stability is breached. The mark *limit* represents the constraint that was used during optimization.

ground impact of the right foot, a short double support phase (highglighted in grey) is used to transfer the body support on the right leg and unload the left foot (6-7). Then the left foot lifts off ground and is retired over the obstacle (7-9). After ground impact of the left foot, the robot enters a re-stabilization phase that ends in a static posture (10-12, highlighted in grey).
The employed problem formulation has the advantage that the motion characteristics (joint trajectories, phase timings, torque profiles) are determined during the optimization process, based on abstract high-level objectives and the governing physics. Phase transitions are determined by implicit switching constraints (a foot may lift off ground as soon as the contact reactions vanish) and discontinuous phase transitions are assumed to be perfectly inelastic (a foot that reaches ground level collides).

C. Equations of Motion

The robot is modeled in minimal coordinates (without contacts) with 30 dof for its internal branched tree structure, 4 dof to account for its elasticity in the ankle, as well as further 6 dof to model the free motion in the global reference. This coordinate configuration is preserved throughout the complete phase cycle featuring position contacts and kinematic loops. The resulting dynamic equation is then expressed as DAE system of index 3 formulated in the so-called descriptor form.

$$M(q,p)\,\ddot{q} + NLE(q,\dot{q},p) + C(q,p) - J(q,p)^T \lambda = \tau \quad (1)$$

$$g(q,p) = 0 \quad (2)$$

In this equation $M(q)$ represents the joint space inertia matrix which consists of the inertia matrix from the kinematic

tree structure of the robot

$$M = \left(\sum_k J_k^T I_k J_k \right) + M_m \tag{3}$$

and an additional diagonal term M_m (4) containing the simplified dynamic effects of the spinning coils in the joint actuators (where I_i^m is the rotational inertia of the coil i about its spinning axis and R_i the ratio of transmission of the joint i):

$$M_{mii} = \begin{bmatrix} R_i^2 I_i^m & i < N \\ 0 & i \geq N \end{bmatrix} \tag{4}$$

$NLE\left(q, \dot{q}\right)$ represents the nonlinear effects (e.g. Coriolis). Furthermore we include here the dynamic effects of the spring and damper systems. The following analysis is based on parameters roughly chosen by hand.

$$NLE = \sum_k J_k^T \left(I_k \dot{J}_k \dot{q} - \dot{q}^T J_k^T \times I_k J_k \dot{q} \right) + K_D \dot{q} + K_p q \tag{5}$$

J_k represent the spatial Jacobian to the local reference frame of the link k respectively. I_k is the spatial inertia matrix of link k. K_D and K_P are matrices that hold spring and damping constants with respect to each of the degrees of freedom [18]

Gravity effects are considered with the term $C\left(q\right)$. τ represents the system's actuation as torque on the joint-level (rotational). The term $g\left(q\right)$ expresses the scleronome position constraints.

For higher computational efficiency, this is transformed into a DAE system of index 1:

$$\dot{q} = v \tag{6}$$

$$\dot{v} = a \tag{7}$$

$$\begin{bmatrix} M & -J^T \\ J & 0 \end{bmatrix} \begin{bmatrix} a \\ \lambda \end{bmatrix} = \begin{bmatrix} -NLE - C + \tau \\ -\gamma \end{bmatrix} \tag{8}$$

In forward dynamics algebraic variables λ (equivalent to the contact constraint forces) and acceleration $\ddot{q}$ values are computed from given system's state $q, \dot{q}, \tau$. Additionally, the following conditions arising from index reduction have to be respected for consistency:

$$g\left(q\left(0\right)\right) = 0 \tag{9}$$

$$J\left(q\left(0\right)\right)\dot{q}\left(0\right) = 0 \tag{10}$$

The term J is the classical (not the spatial!) analytical 6D Jacobian and $\gamma = \frac{\partial}{\partial t}\left(J\right)\dot{q}$ its time derivative multiplied by the velocity vector respectively that contains all active constraint directions in the contact points.

When a foot enters in contact with the ground, this is modeled as an inelastic impact causing discontinuities in the joint velocities which can be computed by the following equation. $\dot{q}^-$ and $\dot{q}^+$ represent the velocity configuration before and after the impact respectively and Λ holds the complex impact impulsion:

$$\begin{bmatrix} M & -J^T \\ J & 0 \end{bmatrix} \begin{bmatrix} \dot{q}^+ \\ \Lambda \end{bmatrix} = \begin{bmatrix} M\dot{q}^- \\ 0 \end{bmatrix} \tag{11}$$

The dynamic equations are composed analytically, optimized and converted into C-code by means of our own dynamic model builder DYNAMOD based on 6D spatial geometry [3]. Inspired by the the work of Wieber [12], the code generation is done building on top of the commercially available package Maple™.

III. Generation of optimal stepping motions by optimal control techniques

In the following the implementation of abstract motion characteristics in the problem formulation will be intensively exploited to generate motions that will rely on the whole body dynamics but at the same time minimize the control effort of the stabilizing algorithm.

A. The optimal control problem

In order to generate the stepping motion over the obstacle, a multiple-phase optimal control problem is formulated (similar to [15]). An optimal control problem is an optimization problem where the unknown variables are functions in time and dynamic equations are respected as constraints. The general formulation (12-19) of this problem uses the time t, the system states $x(t)$, the controls $u(t)$ and system parameters p.

$$\underset{t,x,u,p}{min} \sum_{i=1}^{r} \int_{\bar{t}_{i-1}}^{\bar{t}_i} \Phi_i\left(x(t), u(t), p\right) dt + \Psi_i\left(\bar{t}_i, x\left(\bar{t}_i\right), p\right) \tag{12}$$

$$\text{subject to} \quad \dot{x}(t) - f_i\left(t, x(t), u(t), p\right) = 0 \tag{13}$$

$$x\left(\bar{t}_i^+\right) - h_i\left(x\left(\bar{t}_i^-\right)\right) = 0 \tag{14}$$

$$r_{eq}\left(x(0), T, x(T), \hat{t}_0, x\left(\hat{t}_0\right), ..., \hat{t}_s, x\left(\hat{t}_s, p\right)\right) = 0 \tag{15}$$

$$r_{ineq}\left(x(0), T, x(T), \hat{t}_0, x\left(\hat{t}_0\right), ..., \hat{t}_s, x\left(\hat{t}_s\right), p\right) \geq 0 \tag{16}$$

$$g_i\left(x(t), u(t), p\right) \geq 0 \tag{17}$$

$$\underline{u} \leq u \leq \overline{u} \tag{18}$$

$$\underline{x} \leq x \leq \overline{x} \tag{19}$$

The objective function (12) consists of a continuous Lagrange-term (Φ) and an end time related Meyer-term (Ψ) for each phase. Optimization is done with respect to the system dynamics (13), equality and inequality boundary constraints (15, 16) for all phases, continuous path constraints (17) as well as box-constraints (limits) on system states (19) and controls (18).

$i \in \mathcal{M}$, $\mathcal{M} = \{0...r\}$ regroups all indices of the discrete phases. $\bar{t}_i^+$ and $\bar{t}_i^-$ denote the specific instant of phase transition, the former before and the latter after the phase transition. Without loss of generality it is assumed that $\hat{t}_s = 0$. f_i is the phase dependent right hand side of a first order ODE.

Specifically in this problem formulation the state vector of the system $x = [q, \dot{q}, \tau]^T \in \mathbb{R}^{110}$ comprises joint positions $q \in \mathbb{R}^{40}$ and velocities $\dot{q} \in \mathbb{R}^{40}$ (reduction to first order

ODE) and the joint torques $\tau \in \mathbb{R}^{30}$. The controls $u \in \mathbb{R}^{30}$ are injected into the system as torque derivatives $\dot{\tau}$ to assure continuity of joint torque trajectories during phase transitions. In previous studies this characteristic improved as well the quality of the approximated system input. h_i expresses characteristics of the phase transition $(i-1) \rightarrow (i)$ (e.g. inelastic impact). $f_i, r_{eq}, r_{ineq}, g_i$ are vector functions with correspondent dimension.
Besides the desired final motion characteristics a decision whether a characteristic must be enforced as constrained or objective must be carefully made.

B. Objectives

The objectives are divided into essential (dominant) and overall (sub-dominant) motion characteristics achieved, by individual weights ω_{name} in the objective function.

1) Minimal excitement of ankle elasticity: From the previous presentation (see I-A and II) it is clear that the quality of the backdriveability of the controller is only preserved in the low frequency space, hence allowing only small values for the acceleration and velocity of the corresponding degrees of freedom. As the incorporated elasticity model is only a linear approximation it is only expected to be valid in a small region around the neutral working point:

$$\begin{aligned} \min \Phi_{\text{Elasticity}} = \omega_{Acc} \sum_{i \in \text{Elast}} \ddot{q_i}^2 \\ + \omega_{Vel} \sum_{i \in \text{Elast}} \dot{q_i}^2 + \omega_{Pos} \sum_{i \in \text{Elast}} q_i^2 \end{aligned} \tag{20}$$

2) Minimal linear vertical momentum of CoM: The quality of the simplified modeling of the elasticity may be further improved when excessive oscillation of the vertical force on the elasticity is prevented, as these effects are assumed to be substantially correlated. Furthermore this assumption minimizes the height variations of the CoM and thus deviation from the linear inverted pendulum mode [7] a central assumption of the stabilizer [17].

$$\begin{aligned} \min \Phi_{\text{Linear Momentum}} = \omega_{LinMomZ} \left(L^z_{CoM}\right)^2 \\ + \omega_{\partial LinMomZ} \left(\frac{\partial}{\partial t} L^z_{CoM}\right)^2 \end{aligned} \tag{21}$$

3) Minimal vertical angular momentum change about CoM & vertical contact shear torque: As a motion to dynamically overstep an obstacle may drive the foot contact during single support to its adhesive limits, this objective combination helps at a time to minimize the necessary vertical torque to be canceled in the foot contact and at the same time excessive motions with the upper torso.

$$\min \Phi_{\text{Angular Momentum}} = \omega_{\partial AngMomZ} \left(\frac{\partial}{\partial t} H^z_{CoM}\right)^2 \tag{22}$$

$$\min \Phi_{\text{Contact Torque}} = \omega_{ContactZ} \left(f^{mZ}_{\text{Contact foot}}\right)^2 \tag{23}$$

4) Minimal deviation between whole body ZMP and table cart ZMP: The difference between the whole body ZMP [21] and the 3D-LIPM [17], as it seems to be applied in the stabilization algorithm, is the effect of the change of the horizontal components of the angular momentum about the CoM. These could be used to cancel out the acceleration effect of the CoM about the ground. In the reverse conclusion, it is possible that the optimization tends to exploit this effect to improve the dynamics of the motion, but hence fails to comply with the assumption of the stabilizer. This would risk in a highly unstable motion, a situation that should be avoided if possible. Consequently the euclidean norm of the geometric difference is minimized.

$$\min \Phi_{\text{ZMP - 3D-LIPM}} = \left| ZMP^{x,y}_{\text{whole body}} - ZMP^{x,y}_{\text{Table Cart}} \right|_2^2 \tag{24}$$

5) Minimal performance time: As motion capacities of humanoid robots are still far behind those of humans, it will be interesting to investigate how fast the robot platform HRP-2 is capable to clear the obstacle (in simulation of course) within its strict kinematic and dynamic limits:

$$\min \Psi_{\text{time}} = T_{\text{Global End-time}} \tag{25}$$

6) Head stabilization: In [20] it was reported that angular stabilization of the head and gaze is essential for a dynamic postural control during various manipulation and locomotion tasks. At one hand the desired motion represents a bipedal locomotion problem and at the other hand a tedious postural balance problem. Apart from the fact that HRP-2's IMU is not located in the head, but in the chest [9], is concluded that head stabilization, towards the final target in the global reference frame, is an essential characteristic to improve postural stability as well as the general appearance.

$$\begin{aligned} \min \Phi_{\text{Head}} = (\text{an})_{\text{Yaw}}(x)^2 + \left((\text{an})_{\text{Pitch}}(x) - p_{\text{Pitch-Offset}}\right)^2 \\ + (\text{an})_{\text{Roll}}(x)^2 \end{aligned} \tag{26}$$

7) Minimal variations of squared torques: As stated in [15] it is possible to improve the motion-quality further by minimizing sub-dominantly the squared first derivative of the joint torques. This criteria was mostly integrated for technical reasons (huge control oscillations):

$$\min \Phi_{\text{torque}} = \sum_{j=1}^{30} \left(u_j\right)^2 \tag{27}$$

C. Path constraints

For computational efficiency it is crucial to keep mathematical complexity at the lowest possible level. Besides neglected physical effects, one needs to employ various continuous path constraints to prevent unrealistic physical behavior of the system during the simulation.

1) Foot contact/clearance: As the foot to ground contact is uni-lateral, a valid contact state necessitates pressure in the contact surface. Identification of this condition is done based on the vertical contact constraint force and the *center of pressure* (henceforth called CoP) bound to a subspace of the contact surface [11]. For this analysis the feasible area is reduced to square of 1[cm] x 1[cm] as we will explain in the result section.
Slipping was not explicitly modeled in the foot contact and hence an adequate contact state needs to be enforced. In a first approximation the vertical contact force component is

used to establish a maximal admissible horizontal force component - Coulomb friction cone - and a maximal admissible vertical torque component.
Friction effects are not considered during swing (foot to ground). Consequently a foot clearance is enforced based on a time dependent smooth curve of minimal height of the lowest point of the foot fold to ground distance.

2) Self Collision: An important issue in humanoid robot motion generation is self-collision. As joints are position controlled, unexpected contact during a performed motion usually leads to mechanical deterioration of either the kinematic structure or the concerned actuation system. From the complex kinematic structure the collision free workspace is highly scattered and even during simple dynamic motions, like reaching or walking, self collision between various links is very likely to occur. Additionally possible collisions with the given obstacle, the robot has to step over, need to be avoided. For collision detection a simple line geometry approach based on cylinders [6] but with rounded caps is employed.

3) Pelvis stabilization: In preliminary trials the optimal control problems relayed mainly on the upper torso dynamics to stabilize the whole body motion. As firstly the quality of the dynamic model in the upper torso section is considerably doubted and secondly the effect of a highly dynamic re-orientation of the pelvis section on the stabilizing algorithms is not yet clear, the decision was made to keep roll and pitch orientation in tight angular ranges (-0.005, +0.005) [RAD].

D. Solving optimal control problems

The proposed optimal control problem formulation is solved with the powerful framework MUSCOD II, developed at the University of Heidelberg. Based on early works of Bock and Plitt [1], it has been implemented by Leineweber [10].
The core algorithm consists of a direct multiple shooting method. First a discretization of the system controls into a finite set of additional system parameters is performed, based on an approximation with parametric model functions (piecewise constant/linear, splines) on a given time grid. The choice of the time grid determines the quality governing the approximation of the controls. The system trajectory is further parametrized as a series of initial value problems with additional matching conditions to assure continuity across the multiple shooting intervals. Values for the objective function, boundary and path constraints, including all sensitivities of the trajectory with respect to initial conditions and parameters are then computed through internal numerical differentiation (IND [10]) to allow for high accuracy. Upon this information a large but highly structured general nonlinear program is formulated.
This NLP is then solved based on a sequence of equivalently condensed QP sub-problems [10], where additional parameters of the system trajectory are recursively eliminated. In our set-up, time grids for control and state trajectory discretisation are the same.
Optimization was carried out in a three subsequent steps. First the simulation setup was employed to compute a two step walking motion from static half-sitting posture. As soon as a feasible walking trajectory was found after a few iterations, the obstacle was included in the setup to optimize a stepping motion over the obstacle until a certain obstacle height was reached. Finally the motion was further optimized to form the desired trajectory characteristics.

IV. Results

As the interest of this analysis is not to investigate the maximum obstacle height, but to assess the quality of this approach, optimization has not been tuned towards a maximum obstacle height, but a suitably smooth motion combined with a reasonably obstacle height for safe investigation during real experiments. Thus we chose an obstacle height 20cm (height) x 11cm (width) including safety margin.
The obstacle is successfully cleared in 4.32 [s] (result of optimization), in 4.33 [s] and 4.34 [s] with the virtual robot in simulation and the real robot platform respectively. The optimization freely chooses a step-length of 0.415 [m] and a relatively narrow foot arrangement of 0.17 [m] between feet to clear the obstacle. The robot starts from a nearly symmetric posture and a narrow feet arrangement (0.16 [m] lateral offset, 0.005 [m] sagittal offset) into a slightly larger arrangement to re-stabilize the robot (0.19 [m] lateral offset, 0.09 [m] sagittal offset) into the final static posture (see figure 1 and figure 2). The simulation of the virtual robot and the real experiment showed a smooth motion without slipping, medium ground impact collisions and no destabilizing.
The analysis of the objectives revealed that the optimization converged mostly with desired motion characteristics as dominant objectives: minimum excitement of the ankle elasticity in horizontal and vertical direction, minimal difference between real ZMP and table cart ZMP.
From figure 5 it is clearly observable that the whole body model in our optimization framework, the virtual robot as well as the real robot show relative close motion characteristics. The force/torque control loop only concerns the ground contact reactions Mx, My and Fz. Apart from noise and different initial conditions in the optimization and the simulator OpenHRP the ground contact reactions Fx, Fy, Mz and even Fz closely follow the computed results. Thus it is concluded that perturbation from vertical excitement of the elasticity has been canceled out sufficiently. Contrary Mx and My show large deviation and consequently some chosen motion characteristics of the computed reference need still improvement.
This is further confirmed from figure 6. Deviation from the computed reference during the real experiment and even the simulation are clearly observable in the ankle joint as well as in the knee joint of both legs. This verifies as well the aspect that the whole lower body is used to apply the manipulation of the trajectories of the stabilizer. Besides these deviations, the overall trajectories coincide relatively well most of the time. Furthermore the deviation of the posture control, visible in the global orientation of the torso stays small (see figure 4). Thus we conclude, that our employed

strategy was successful, despite, modeling errors (elasticity, mass distribution) and the reference trajectory, that seem not to be fully compatible with the stabilizing algorithms, but hence has even to account for potential differences between simulation and real robot (see figure 6 red mark).
A comparison between figure 3 and 7 reveals an interesting fact. Figure 3 shows deviations between the real ZMP and the Table Cart ZMP (as this objective was not triggered to be the first dominant one - these deviations are reasonable). Apart from the high peaks during the phase transitions (single support $\leftrightarrow$ double support) a high correlation between the deviations in figure 3 and 7. Same tendency is visible on figure 5 (see plot My !). Even though the CoP was constrained to move only in a squared area of 1 [cm] x 1 [cm] (blue line), the final result of the stabilizer moves the CoM in a much larger area of approximately 10 [cm] x 10 [cm], which is however still compatible with the geometry of the foot (see figure 7). Besides simplifications in the modeling of the elasticity, this might give evidence about the stabilizing algorithm following the table cart ZMP reference [17]. The local CoP in the left foot - especially during single support - moves to the opposite direction of the observable deviation between the real and the table cart ZMP. Thus the stabilizing algorithm seems to not account for the dynamic compensation based on the angular momentum and consequently deviates from the computed reference.

V. CONCLUSIONS & PERSPECTIVE

This paper proposes a new generic strategy to investigate the hardware and control limits of a given robotic platform based on a dynamically challenging motion. This strategy massively exploits the possibility to formulate desired abstract motion characteristics based on high-level objectives. Despite unavoidable modeling errors and small incompatibility of our computed reference trajectories to the stabilizing algorithms, the real robotic platform was still able to safely operate during the motion performance.
Based on the previous analysis further adjustments to the formulation of desired motion characteristics should lead to a more predictable behavior of the motion control and stabilizing algorithms, to investigate the actual li¡mits even more precisely. Future prospects will be further refinements to the whole body dynamics model as well as extension to other dynamically challenging motions, such as dynamically stepping through a narrow passage.

ACKNOWLEDGMENT

Financial support of HGS MathComp and the KOROIBOT Project for this work is gratefully acknowledged. We thank the SimOpt team (Hans Georg Bock) of the University of Heidelberg for providing the optimal control code MUSCOD. The authors would like to thank as well Maximilien Naveau for his valuable help during the experiment-phase on the HRP-2 robot.

REFERENCES

[1] H. Bock and K. Plitt. A multiple shooting algorithm for direct solution of optimal control problems. pages 243–247. Pergamon Press, 1984.

[2] B.Verrelst, K.Yokoi, O.Stasse, H.Arisumi, and B.Vanderborght. Mobility of humanoid robots: Stepping over large obstacles dynamically. In *IEEE International Conference on Mechatronics and Automation (ICMA)*, 2006.

[3] R. Featherstone. *Rigid Body Dynamics Algorithms*. Springer-Verlag New York, Inc., Secaucus, NJ, USA, 2007.

[4] H.Hirukawa, F.Kanehiro, K.Kaneko, S.Kajita, K.Fujiwara, Y.Kawai, F.Tomita, S.Hirai, K.Tanie, T.Isozumi, K.Akachi, T.Kawasaki, S.Ota, K.Yokoyama, H.Handa, Y.Fukase, J.-I.Maeda, Y.Nakamura, S.Tach, and H.Inoue. Humanoid robotics platforms developed in hrp. *Robotics and Autonomous Systems*, 48:165–175, 2003.

[5] J.Englsberger, C.Ott, and A.Albu-Schffer. Three-dimensional bipedal walking control using divergent component of motion. In *IEEE/RSJ International Conference on Intelligent Robots and Systems (IROS)*, 2013.

[6] J.S.Ketchel and P.M.Larochelle. Collision detection of cylindrical rigid bodies using line geometry. In *IDETC/CIE ASME International Design Engineering Technical Conference & Computers and Information in Engineering Conference*, 2005.

[7] S. Kajita, F. Kanehiro, K. Kaneko, K. Fujiwara, K. Harada, K. Yokoi, and H. Hirukawa. Biped walking pattern generation by using preview control of zero-moment point. In *IEEE/RAS Int. Conf. on Robotics and Automation (ICRA)*, 2003.

[8] S. Kajita, T. Nagasaki, K. Kaneko, and H. Hirukawa. Zmp-based biped running control. *IEEE Robotics and Automation Magazine*, 07:63–73, 2007.

[9] K. Kaneko, F. Kanehiro, S. Kajita, H. Hirukawaa, T. Kawasaki, M. Hirata, K. Akachi, and T. Isozumi. Humanoid robot HRP-2. In *IEEE/RAS Int. Conf. on Robotics and Automation (ICRA)*, 2004.

[10] D. Leineweber, I. Bauer, H. Bock, and J. Schlder. An efficient multiple shooting based reduced SQP strategy for large-scale dynamic process optimization - Part I: theoretical aspects. pages 157 – 166. 2003.

[11] O.Ramos, L.Saab, S.Hak, and N.Mansard. Dynamic motion capture and edition using a stack of tasks. In *Proceedings of the IEEE-RAS International Conference on Humanoid Robots*, 2011.

[12] P.-B.Wieber, F.Billet, L.Boissieux, and R.Pissard-Gibollet. The humans toolbox, a homogenous framework for motion capture, analysis and simulation. In *International Symposium on the 3D Analysis of Human Movement*, 2006.

[13] P.Michel, J.Chestnutt, J.Kuffner, and T.Kanade. Vision-guided humanoid footstep planning for dynamic environments. In *Proceedings of the IEEE-RAS International Conference on Humanoid Robots*, 2005.

[14] L. Roussel, C. C. de Wit, and A. Goswami. Generation of energy optimal complete gait cycles for biped robots. In *IEEE/RAS Int. Conf. on Robotics and Automation (ICRA)*, 1998.

[15] G. Schultz and K. D. Mombaur. Modeling and optimal control of human-like running. *IEEE/ASME Transactions on Mechatronics*, 15:783–792, 2010.

[16] S.Kajita, K.Yokoi, M.Saigo, and K.Tanie. Balancing a humanoid robot using backdrive concerned torque control and direct angular momentum feedback. In *IEEE/RAS Int. Conf. on Robotics and Automation (ICRA)*, 2001.

[17] S.Kajita, T.Nagasaki, K.Kaneko, K.Yokoi, and K.Tanie. A running controller of humanoid biped hrp-2lr. In *IEEE/RAS Int. Conf. on Robotics and Automation (ICRA)*, 2005.

[18] S.Nakaoka, S.Hattori, F.Kanehiro, S.Kajita, and H.Hirukawa. Constraint-based dynamics simulator for humanoid robots with shock absorbing mechnisms. In *IEEE/RSJ International Conference on Intelligent Robots and Systems (IROS)*, 2007.

[19] T.Erez and E.Todorov. Trajectory optimization for domains with contacts using inverse dynamics. In *IEEE/RSJ International Conference on Intelligent Robots and Systems (IROS)*, 2012.

[20] T.Pozzo, Y.Levik, and A.Berthoz. Head and trunk movements in the frontal plane during complex dynamc equilibrium tasks in humans. *Experimental Brain research*, 106:327 – 338, 1995.

[21] M. Vukobratovic and J. Stephanenko. On the stability of anthromomorphic systems. *Mathematical Biosciences*, 15:1–37, 1972.

[22] Y.Guan, K.Yokoi, and K.Tanie. Feasibility: Can humanoid robots overcome given obstacles. In *IEEE/RAS Int. Conf. on Robotics and Automation (ICRA)*, 2005.

[23] Y.Xiang, J.S.Arora, and K.Abdel-Malek. Physics-based modeling and simulation of human walking: a review of optimization-based and other approaches. *Medical and Bioengineering Application*, 42:1–23, 2010.